

**1 of 1**

SAND--93-0240  
Conf-9307124--1

## BINDING OF COPPER TO NANOCAVITY SURFACES IN SILICON

S. M. MYERS, D. M. FOLLSTAEDT AND D. M. BISHOP

Sandia National Laboratories, Albuquerque, New Mexico 87185 U.S.A.

Keywords: silicon, copper, gettering, ion implantation, cavities

### ABSTRACT

We demonstrate that nanometer-scale voids within Si, formed by He ion implantation and annealing, trap Cu atoms with a binding energy of  $2.2 \pm 0.2$  eV relative to solution. This trapping saturates at a level consistent with monolayer coverage of the cavity walls, and it is ascribed to the reaction of Cu with Si dangling bonds on the internal surfaces. Our experiments also confirm the previously reported solution enthalpy of Cu in Si relative to precipitated  $\text{Cu}_3\text{Si}$ , 1.7 eV, so that the binding at cavity traps is stronger. It is proposed that nanocavities may provide superior gettering of metallic impurities in Si.

### INTRODUCTION

Ion implantation of He into Si at room temperature and a concentration of several atomic percent produces a high density of nanometer-size bubbles localized near the implantation range. Subsequent annealing in vacuum above about 900 K induces diffusion of the He from the cavities, leaving behind empty voids. During heating the cavities also become larger and develop facets, and there is extensive annealing of implantation damage [1-3]. The internal surfaces of these cavities are expected to contain approximately one monolayer of Si dangling bonds with high chemical reactivity, and this was previously confirmed through observation of strong H trapping at the dangling bonds [3-5].

In the present work we investigated the interaction of Cu with implantation-formed cavities in Si. When present as contaminants, Cu and the other transition metals are detrimental to the electrical properties of Si devices at concentrations as low as  $10^{-10} \text{ nm}^{-3}$  ( $10^{11} \text{ cm}^{-3}$ ). Therefore, an internal-surface chemisorption reaction sufficiently strong to remove such dilute impurities from solution is of technological as well as scientific interest. This is especially so if the binding reaction is stronger than that in the metal silicides, whose precipitation at deliberately introduced nucleation sites is currently the basis of most impurity gettering in Si devices [See, e.g., Ref. 6].

Our objective was first to establish the occurrence of Cu trapping at cavities in Si and then to determine the binding energy and the number of trapping centers in relation to the cavity-wall surface area. This was accomplished by ion-implanting He and Cu to form multiple layers at different depths containing either cavities or Cu-silicide precipitates, and then observing the redistributions of Cu among these layers during vacuum annealing. Transmission electron microscopy (TEM) was employed to image cavity microstructures and identify the silicide phase, while the depth profile of Cu was monitored nondestructively by Rutherford backscattering spectrometry (RBS). The binding energies of the Cu in cavity traps and  $\text{Cu}_3\text{Si}$  precipitates were then extracted by fitting diffusion-trapping theory to the observed thermally induced internal redistributions.

### RESULTS AND ANALYSIS

A typical cavity layer is shown in the cross-section TEM micrograph of figure 1. In this instance He

MASTER

REPRODUCTION OF THIS DOCUMENT IS UNLIMITED

was ion-implanted at 30 keV to a fluence of  $1000 \text{ nm}^{-2}$  ( $10^{17} \text{ cm}^{-2}$ ), and the specimen was subsequently annealed for 30 min at 973 K. The cavities are seen to lie within the approximate depth interval 150-350 nm, consistent with the predicted depth distribution of the implanted He [7].

The average

diameter of the cavities is 8 nm. Detailed analysis of this and other micrographs indicates that there is  $6.7 \pm 1.2 \text{ nm}^2$  of cavity-wall surface area per  $\text{nm}^2$  of external surface, implying approximately 50 internal-surface dangling bonds per  $\text{nm}^2$  of external surface. Post-implantation annealing at the higher temperature of 1073 K caused the cavities to be larger, about 12 nm, and fewer in number leading to a somewhat reduced total area.

Trapping of Cu by a cavity layer like that of figure 1 was demonstrated by ion-implanting  $1000 \text{ Cu/nm}^2$  at 150 keV into the *opposite* side of the 0.25-mm-thick Si wafer and then performing a series of vacuum anneals at 1073 K. This caused precipitation of  $\text{Cu}_3\text{Si}$  in accord with the Si-Cu phase diagram, as indicated by transmission electron diffraction; in particular, rings and arcs were observed that correspond to intense reflections of  $\eta\text{-Cu}_3\text{Si}$  [8]. The precipitation was followed over longer times by partial dissolution of the silicide and diffusion of Cu *across the wafer* to the cavities. The progressive accumulation of Cu within the cavity layer was observed by RBS and is plotted as open circles in figure 2. The transfer is seen to saturate at about  $50 \text{ Cu/nm}^2$ , consistent with the number of wall dangling bonds estimated from TEM. The saturation depth profile of Cu is given by the open circles in figure 3, and it is consistent with the cavity distribution in figure 1. The number of cavities resulting from 30-keV He implantation decreased rapidly with decreasing fluence, being several times smaller at  $200 \text{ He/nm}^2$  and negligible at  $100 \text{ He/nm}^2$ , and the quantity of trapped Cu declined correspondingly, as seen from the three saturation profiles in figure 3. These results indicate that Cu is

Figure 1. Cross-section TEM of cavities in Si.

Figure 2. Diffusion of Cu from  $\text{Cu}_3\text{Si}$  precipitates to cavity traps.

bound more stably at cavity traps than in the precipitated silicide.

Diffusion of Cu from precipitated silicide to cavity traps was also observed over a much smaller distance, and at a lower temperature, by introducing both layers on the same side of the Si wafer. In this experiment,  $1000 \text{ He/nm}^2$  was implanted at 100 keV yielding a calculated mean range of 680 nm [7], and  $1000 \text{ Cu/nm}^2$  was implanted at 150 keV to achieve a range of 110 nm. In this way the diffusion distance was decreased from  $250 \mu\text{m}$  to  $<1 \mu\text{m}$ . The subsequent isothermal annealing was performed at 723 K, and the resulting transfer of Cu as measured by RBS is given by the filled circles in figure 2.

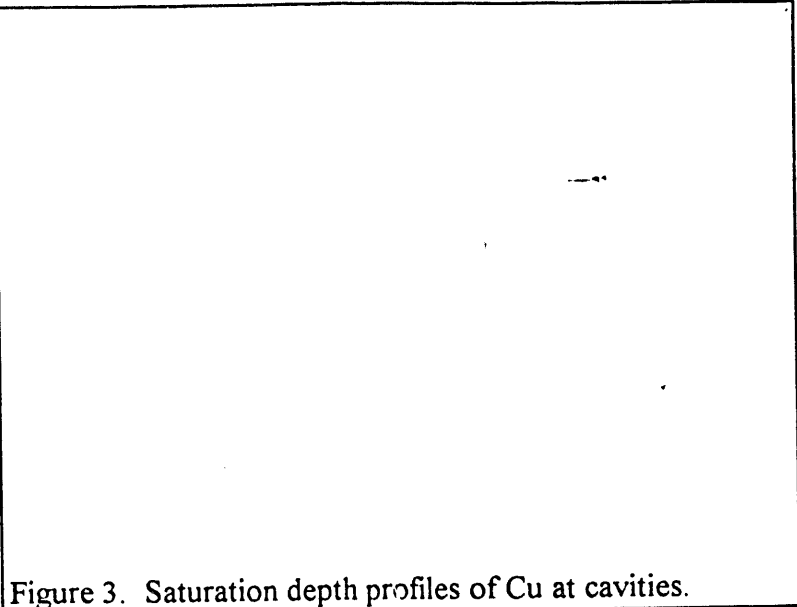


Figure 3. Saturation depth profiles of Cu at cavities.

The curves through the data in figure 2 represent fitted numerical solutions of the formalism for solute diffusion accompanied by trapping and second-phase precipitation [9]. In these calculations the Cu diffusion coefficient was taken from the literature [10], the areal density of cavity-wall trapping sites was adjusted to conform to the observed saturation in figure 2, and the solid-solubilities of Cu in equilibrium with  $\text{Cu}_3\text{Si}$  at 723 and 873 K were adjusted to produce agreement with the data. The binding energy at the cavity traps, expressed relative to Cu in solution, was equated to the value obtained below, 2.2 eV. For these particular experiments, however, essentially the same result would be obtained by assuming the trapping to be irreversible. The physical basis of the calculations can be conveyed by noting that the transfer of Cu occurs under conditions of very nearly steady-state diffusion, so that in a simplified treatment the flux,  $\Phi$ , is given by

$$\Phi \approx n_0 D / \Delta x \quad (1)$$

where  $n_0$  is the solubility expressed as an atomic density,  $D$  is the diffusion coefficient, and  $\Delta x$  is the separation of the two layers. The slight curvature of the more rigorously calculated curve for the smaller separation arises from the fact that, due to the non-zero widths of the two layers, there is a range of diffusion distances.

The Cu solubilities obtained from the above analysis are  $1.7 \times 10^{-9} \text{ nm}^{-3}$  at 723 K and  $2.0 \times 10^{-7} \text{ nm}^{-3}$  at 873 K. This temperature dependence corresponds to an activation energy of 1.73 eV. Previously, thermodynamic equilibrium between macroscopic quantities of  $\text{Cu}_3\text{Si}$  and Si was examined at temperatures above 923 K, giving  $n_0 = (6600 \text{ nm}^{-3}) \exp(-1.744 \text{ eV}/kT)$  [11]. When extrapolated, these results yield solubilities at 723 and 873 K that are, respectively, 2.7 and 2.8 times larger than our values at the two temperatures. Since the extrapolation extends over three orders of magnitude, and since our determination of the solubility is dependent on the value of the diffusion coefficient used, this agreement is considered satisfactory.

The binding energy of Cu within cavity traps was determined from observations of Cu redistribution between two cavity layers, one initially saturated with Cu and the other initially unoccupied. In considering these experiments it is useful to refer to figure 4, which contains RBS depth profiles of the Cu at key points. Helium was first implanted at 100 keV to a fluence of  $1000 \text{ nm}^{-2}$  and the

specimen then annealed for 30 min at 973 K, producing a cavity layer centered at a depth of approximately 680 nm. Copper was subsequently implanted at 150 keV to a fluence of  $100 \text{ nm}^{-2}$ , forming a Cu-rich zone extending from the surface to about 150 nm, as seen from the depth profile given by crosses in figure 4. An anneal of 3 h at 1073 K followed, which served to saturate the cavity traps and also to evaporate most of the excess Cu from the specimen, as seen from the profile given by open circles.

The next step was to introduce a second, unoccupied cavity layer at a depth of approximately 300 nm, which was accomplished by implanting  $1000 \text{ He/nm}^2$  at 30 keV and annealing for 30 min at 973 K. Finally, a series of anneals at 973 K caused the Cu to diffuse from the first to the second cavity layer until the occupancies of the trapping sites reached mutual equilibrium. This final condition is seen in the profile given by filled circles in figure 4. The fact that the two Cu peaks do not have equal area is attributed to the higher anneal temperature of 1073 K experienced by the first, deeper layer; this higher temperature is known to diminish the internal surface area somewhat through cavity agglomeration.

The transfer of Cu from the first cavity layer to the second at 973 K is shown in fig. 5, along with data for a similar anneal sequence at 923 K. (The zero-time areal density is lower for 973 K than 923 K because the transfer during the 30-min cavity-forming anneal at 973 K was included in the first plot but not the second.) The curves represent numerical solutions of the previously cited diffusion-trapping theory, with the diffusion coefficient again being taken from the literature and the cavity-trap binding energy being adjusted to produce agreement with experiment. The binding

energy can actually be obtained from data taken at only one temperature, but achieving consistency between two temperatures provides reinforcement. A physically illuminating simplification of our analysis is achieved by assuming that the layers have zero width and that the Cu diffuses under nearly steady-state conditions. The Cu flux is then given by

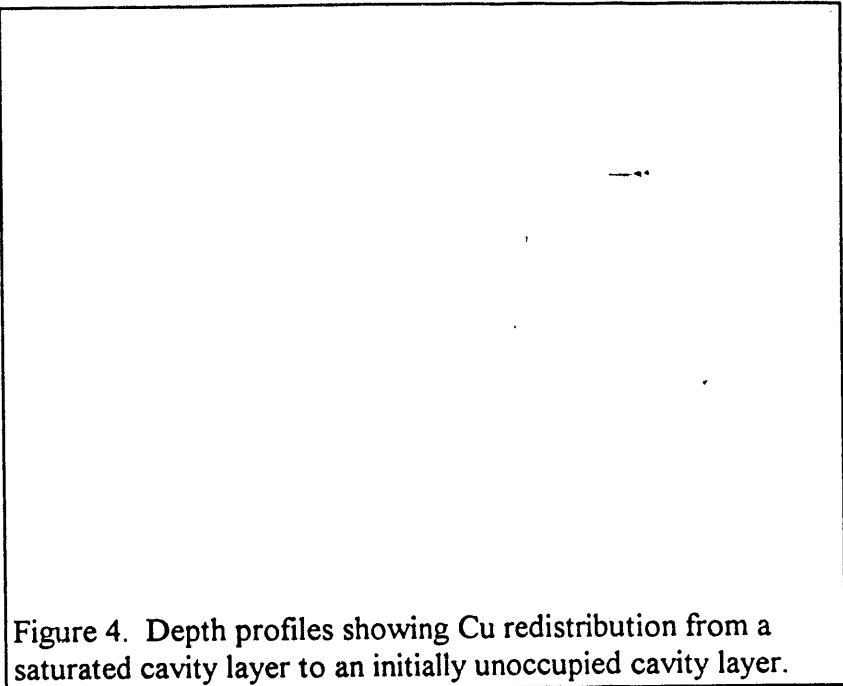


Figure 4. Depth profiles showing Cu redistribution from a saturated cavity layer to an initially unoccupied cavity layer.

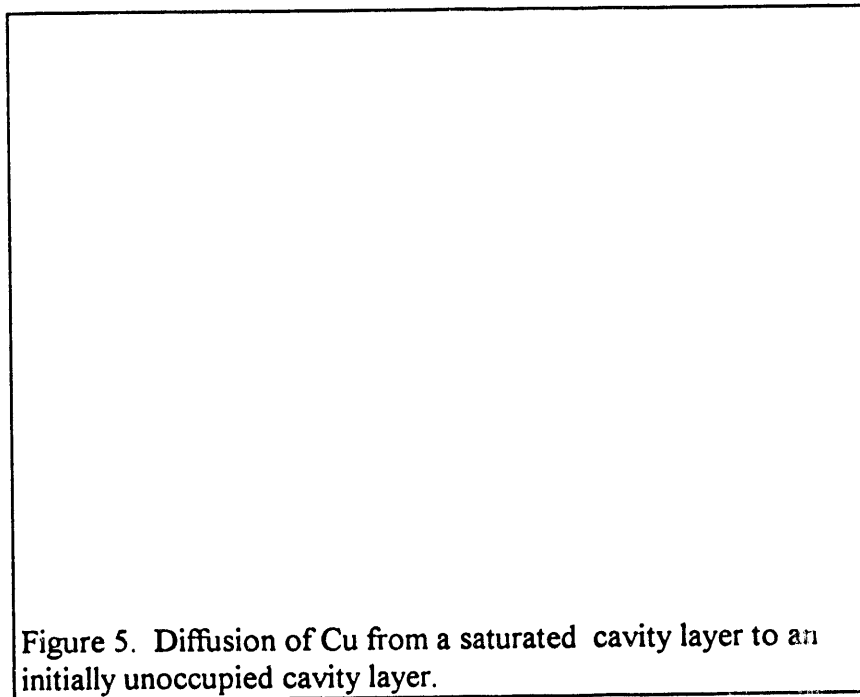


Figure 5. Diffusion of Cu from a saturated cavity layer to an initially unoccupied cavity layer.

$$\Phi \approx [n_c(\theta_1) - n_c(\theta_2)]D/\Delta x \quad (2)$$

where  $n_c(\theta)$  is the solution concentration in *local* equilibrium with the traps. This latter quantity depends on the fractional occupancy of the trapping sites,  $\theta$ , according to the relation

$$n_c(\theta)/N_s \approx [\theta/(1-\theta)]\exp(-E_c/kT) \quad (3)$$

where  $N_s$  is the atomic density of solution sites and  $E_c$  is the trap binding energy relative to solution. Hence the experimentally measured flux  $\Phi$  is very sensitive to the binding energy.

The theoretical fitting shown in figure 5 yields a cavity-trap binding energy of  $2.2 \pm 0.2$  eV relative to Cu in solution. This is 0.5 eV greater than the binding energy in the silicide phase, indicating that the trapping at internal surfaces is strongly preferred.

## IMPLICATIONS

Cavities formed in Si by He ion implantation have several properties which favor their use for gettering of metallic impurities. First, the presence of Si dangling bonds protruding unobstructed into the overlying void should lead to high chemical reactivity, and this is borne out by the present work. Indeed, the binding energy for Cu impurities at cavities was demonstrated to be substantially larger than that in the equilibrium silicide, and the cavities even induced dissolution of the silicide phase from the opposite side of the wafer. A second point is that the cavities are stable at the temperatures of device processing, undergoing some enlargement and coalescence but remaining localized within the implanted layer to at least 1373 K. The use of a trapping process rather than second-phase formation for gettering should also be inherently advantageous, since trapping persists to arbitrarily small concentrations instead of ceasing at a characteristic solid solubility. Finally, because the cavity-trapping process is accomplished by inert-gas ion implantation and annealing, it should facilitate front-side as well as back-side gettering. Still to be established by further research, however, are the actual strengths of the trapping reaction for the other important metallic impurities.

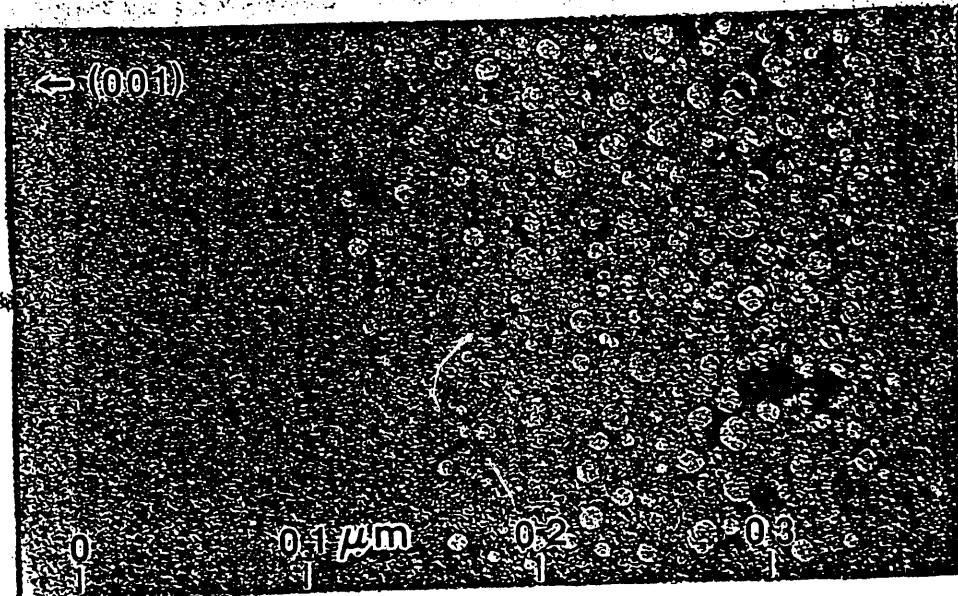
## REFERENCES

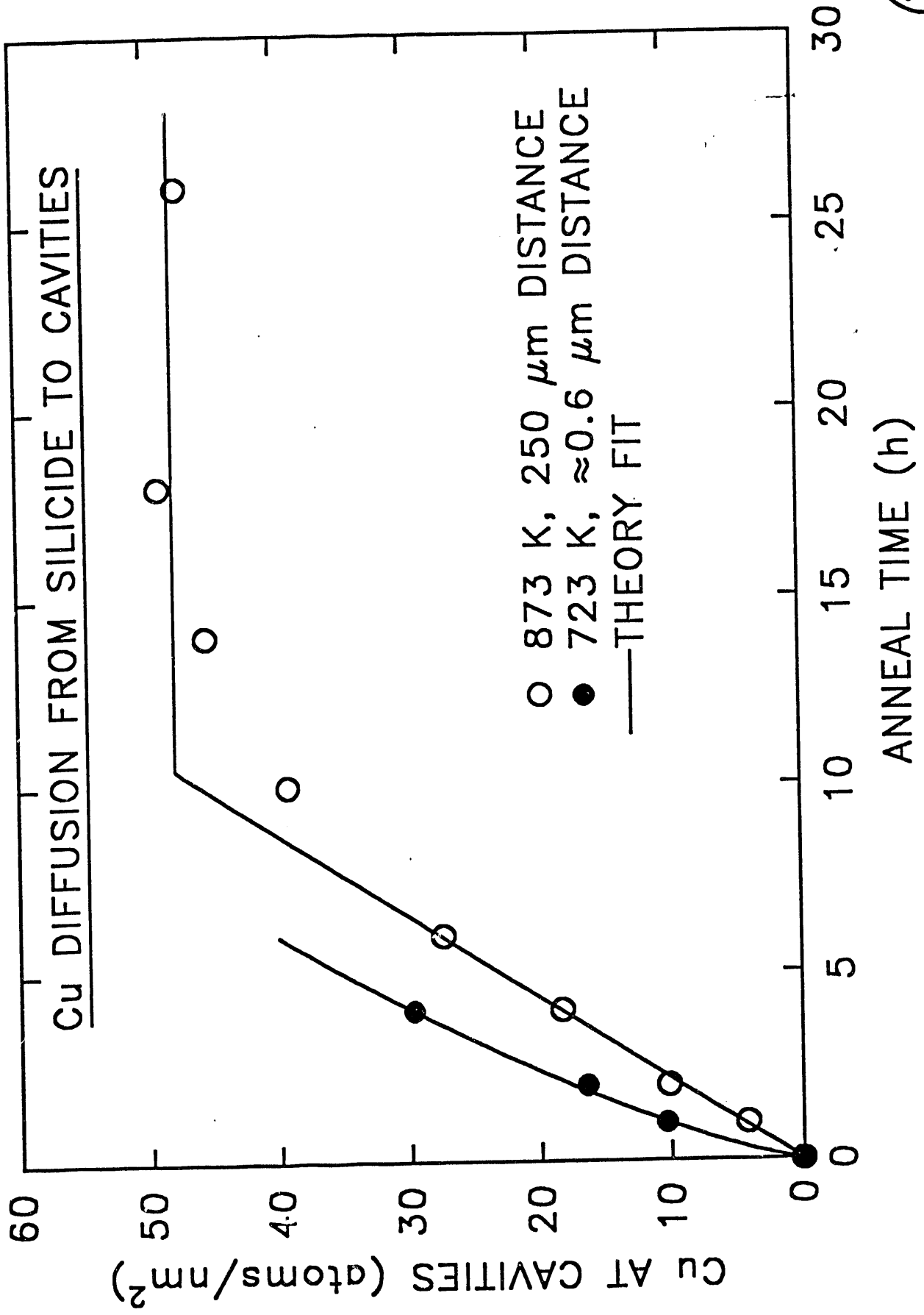
- 1) Griffioen, C.C., Evans, J.H., De Jong, P.C., and Van Veen, A.: Nucl. Instrum. Meth. B, 1987, 27, 417.
- 2) Follstaedt, D.M.: Appl. Phys. Lett., 1993, 62, 1116.
- 3) Myers, S.M., Follstaedt, D.M., Stein, H.J., and Wampler, W.R., Phys. Rev. B, 1993, 47, 13380.
- 4) Stein, H.J., Myers, S.M., and Follstaedt, D.M.: J. Appl. Phys., 1993, 73, 2755.
- 5) Wampler, W.R., Myers, S.M., and Follstaedt, D.M.: Phys. Rev. B, 1993, in press.
- 6) Graff, K.: Mater. Sci. Eng. B, 1989, 4, 63.
- 7) Ziegler, J.F., Biersack, J.P., and Littmark, U.: The Stopping and Range of Ions in Solids, vol. 1 (Pergamon, New York, 1985).
- 8) Powder Diffraction File, Inter. Center for Diffraction Data, Swarthmore, Penn. File No. 23-224.
- 9) Myers, S.M., and Follstaedt, D.M.: J. Appl. Phys., 1989, 65, 311.
- 10) Hall, R.N.: J. Appl. Phys., 1964, 35, 379.
- 11) Dorward, R.C., and Kirkaldy, J.S.: Trans. Metall. Soc. AIME, 1968, 242, 2055.

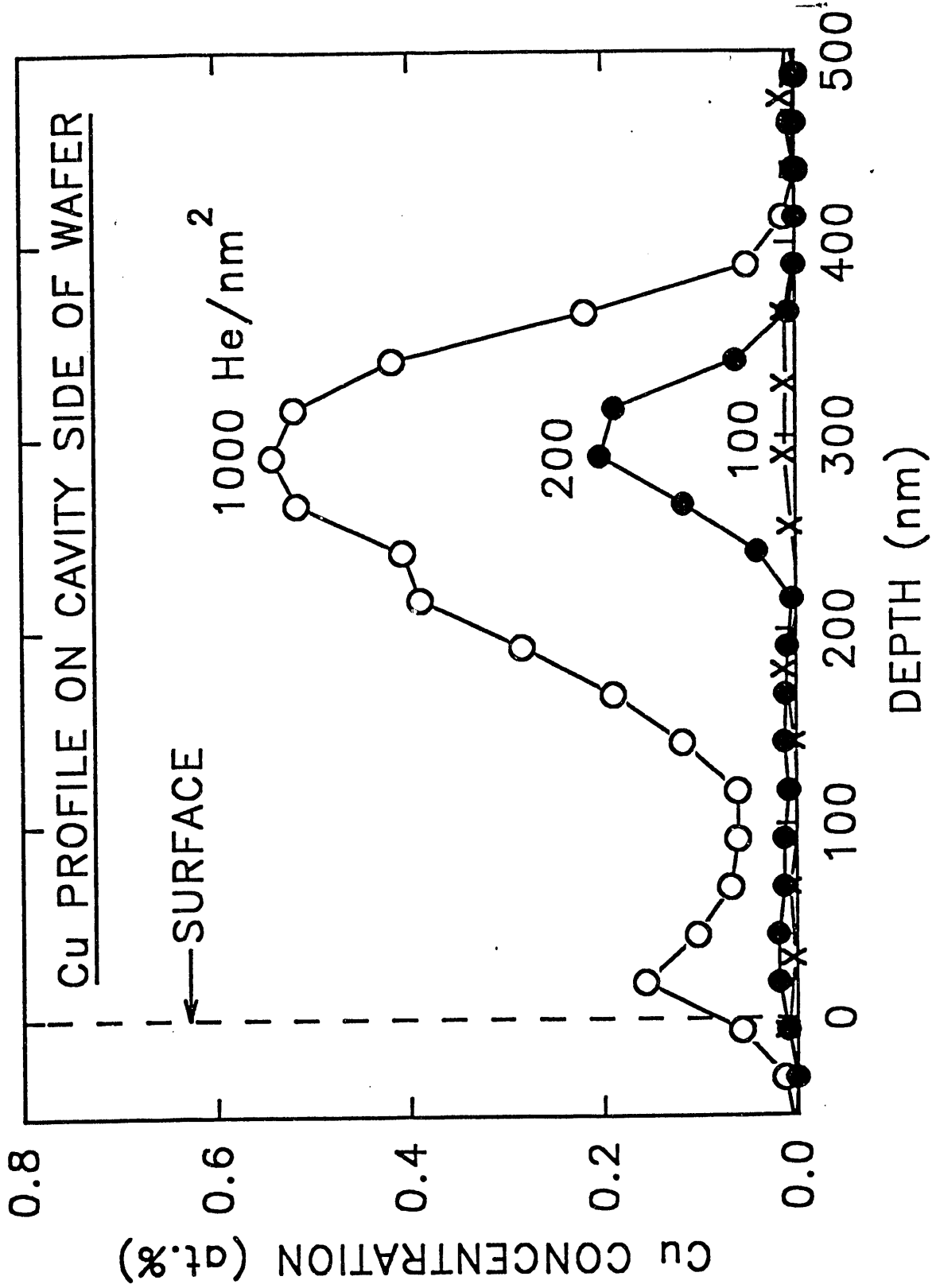
## ACKNOWLEDGEMENTS

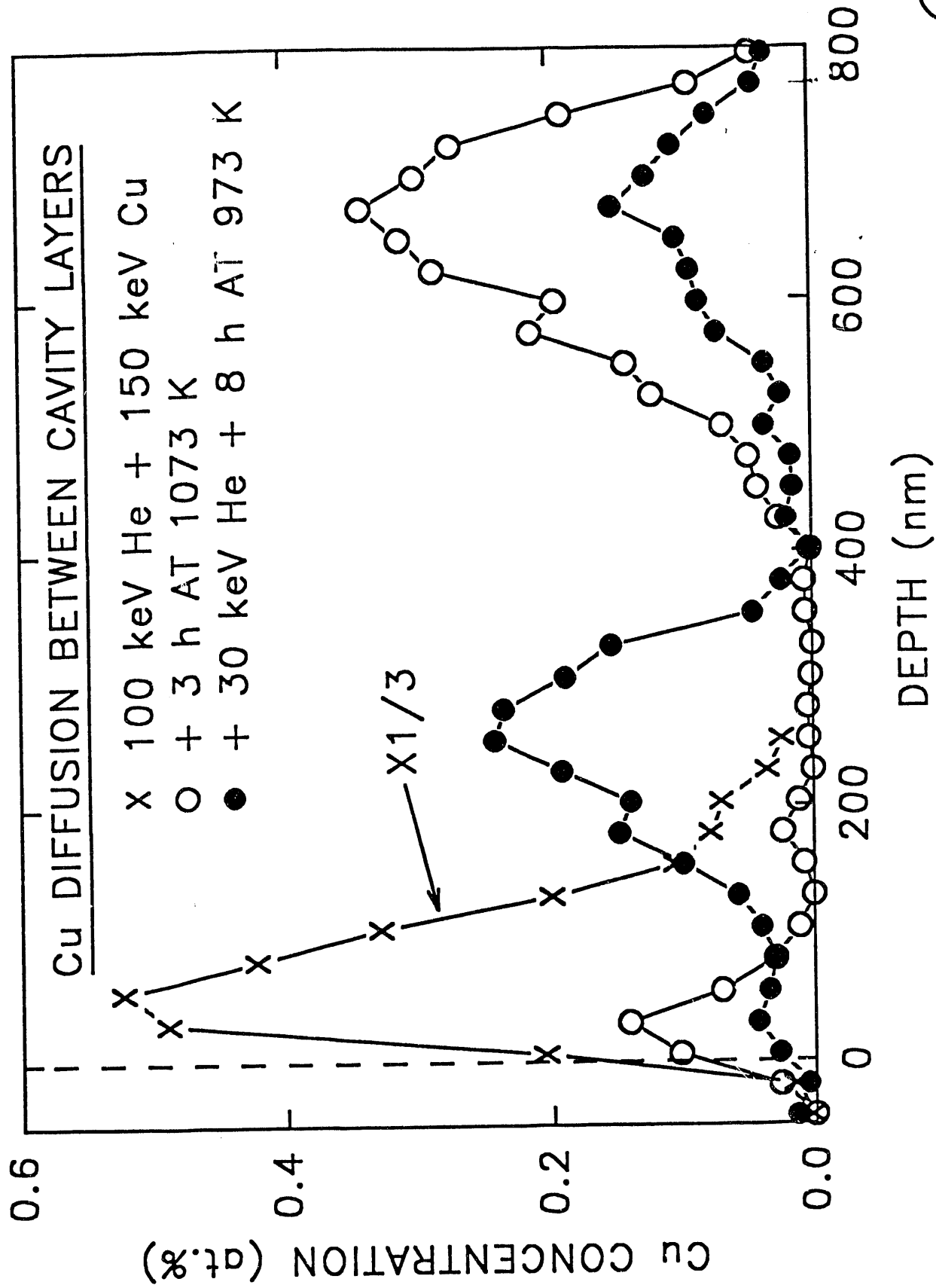
The authors are pleased to acknowledge key discussions with H. J. Stein that led to this investigation. The work was funded by the U.S. Dept. of Energy, Office of Basic Energy Sciences, Div. of Materials Sciences, under Contract No. DE-AC04-76DP00789.

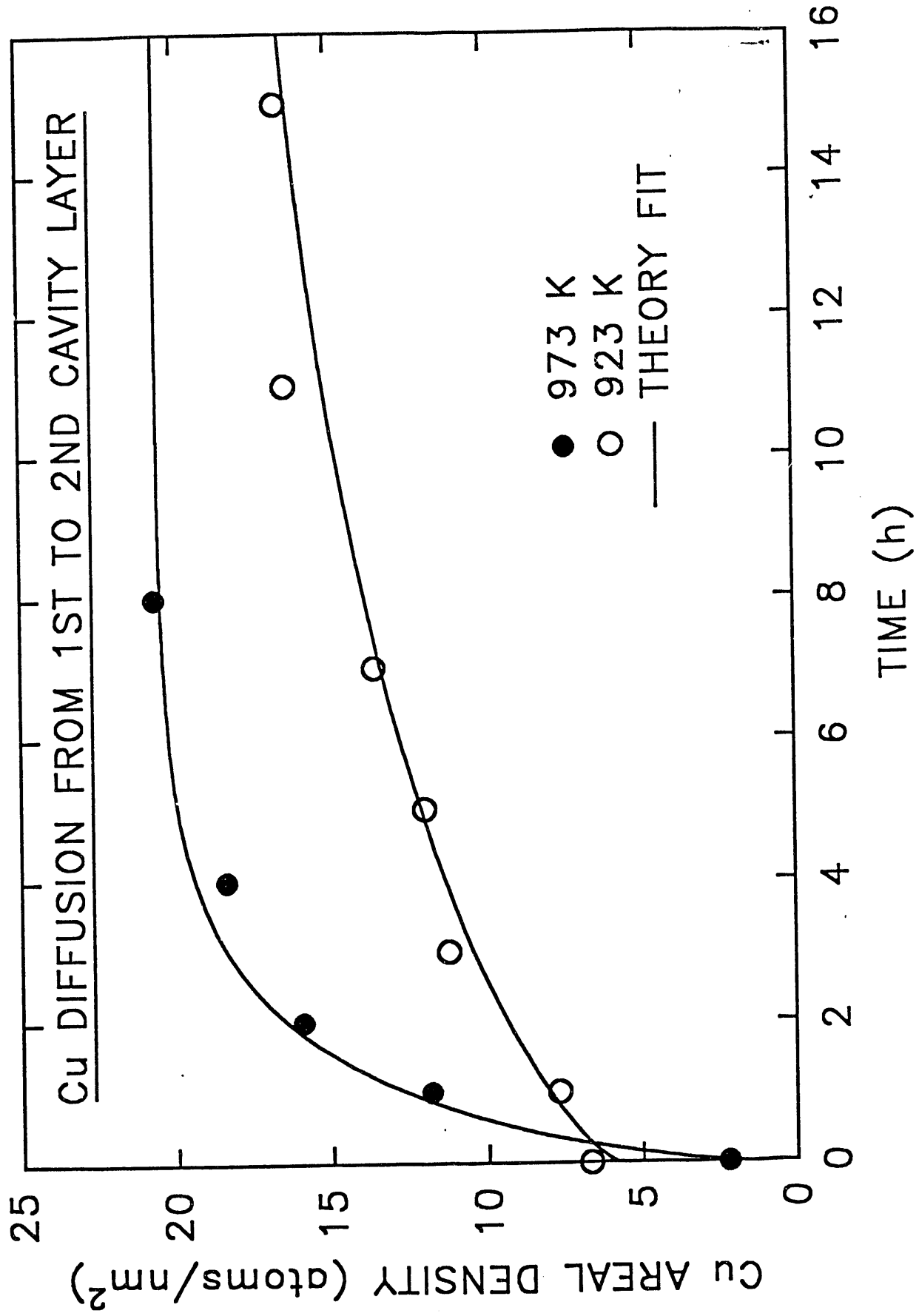
①











**DATE  
FILMED**

*10 / 19 / 93*

**END**